Fusion Engineering and Design 8 (1989) 173–179
North-Holland, Amsterdam

EXAMINATION OF MHD FLUID FLOW IN GEOMETRIC ELEMENTS OF A FUSION REACTOR BLANKET USING THE CORE FLOW APPROACH

M.S. TILLACK

Mechanical, Aerospace and Nuclear Engineering Department, University of California, Los Angeles, Los Angeles, CA 90024-1597 USA

The attractiveness of liquid metal blankets depends strongly on the degree of which peak pressures and temperatures can be controlled. These, in turn, are determined by the MHD pressure drop and velocity field. Accurate methods of predicting the pressure drop, velocity and temperature profiles in liquid metal blankets are necessary for blanket design and for planning and analysis of experiments.

The governing equations for MHD fluid flow are well known. However, solution of the full set of MHD equations is difficult in some geometries and parameter ranges of interest. In many cases, the most important MHD effects can be accurately modeled using a simplified approach, known as the "core flow approximation", which neglect inertial and viscous terms.

A core flow solution method has been developed utilizing the special properties of the MHD equations to reduce them to, at most, four two-dimensional partial differential equations. The method has been formulated in a very general way, to allow treatment of problems with three-dimensional magnetic field and complex channel shapes.

Solutions have been obtained numerically for several cases of interest to fusion. These include conducting pipes with variable radius, variable transverse magnetic field strength, and arbitrary angle of the field with respect to the flow direction. Initial analysis has focused on localized perturbations, including expansions, contractions, and magnetic field entrance/exit regions. Benchmarking has been performed in cases for which data exist. The results indicate that the method is very powerful and could be generalized to treat most geometric elements of liquid metal blankets and high heat flux components.

1. Introduction

Some of the largest remaining uncertainties in liquid metal blanket behavior result from uncertainties in MHD fluid flow in complex blanket geometries and magnetic fields. One of the reasons these uncertainties are difficult to resolve stems from the complexity of the full set of MHD equations.

In many cases, the most important MHD effects can be accurately modeled by using a simplified approach, known as the "core flow approximation". Under sufficiently high magnetic fields, inertial and viscous forces become small. Neglecting these, and assuming small magnetic Reynolds number, a linear set of equations results, including Ohm's law, the simplified momentum equation, and conservation of mass and current.

A solution method is described here based on direct integration of the MHD equation along magnetic field lines, as first suggested by Kulikovskii [1]. The approach uses the special properties of the MHD equations to reduce them to, at most, four two-dimensional partial differential equations. The solution has been formulated in a very general way, to allow the solution of problems with three-dimensional magnetic field and complex channel shapes.

In some cases, the core equations alone can not adequately describe the full details of the velocity profiles in ducts. Care must be exercised in order to properly account for inertial and viscous effects, or to demonstrate that they can be neglected. For example, the no-slip condition (zero velocity at the walls) leads to narrow boundary layers in which viscous forces are comparable with the MHD force. These are the Hartmann boundary layers. In the cases treated here, the walls are conducting, such that the Hartmann layers carry negligible current. Thus, their effect on the core velocity and pressure fields is negligible.

Geometrical or electrical constraints my lead to viscous boundary layers, internal (or "free shear") layers, or inertial layers. A survey of these MHD layers can be found in refs. 2–4. In the circular pipe problems treated here, the boundary conditions present no special problems except at the point where the field is tangent to the wall. Because this occurs only at a point, the problem

can be resolved. In general, if the walls are smooth, have finite conductivity, and are not exactly parallel to the magnetic field, then the current and flow quantity in boundary layers are small.

Finally, at sufficiently low values of the magnetic field, the magnetic force diminishes and the core flow approximation because invalid. The criteria which specify the valid range of application of this method are not fully known, except in the simplest geometries.

2. Description of the direct integration method

The equations describing liquid metal MHD fluid flow include both Maxwell's equations and the Navier–Stokes equation. In dimensionless form, the Navier–Stokes equation is expressed as:

$$\frac{1}{N}(\boldsymbol{v}\cdot\nabla)\boldsymbol{v} = -\nabla p + \boldsymbol{J}\times\boldsymbol{B} + \frac{1}{\mathrm{Ha}^2}\nabla^2\boldsymbol{v}. \tag{1}$$

The MHD body force is given by $\boldsymbol{J}\times\boldsymbol{B}$, and the two dimensionless groups describing the relative magnitude of the terms are the Hartmann number (Ha) and the interaction parameter (N);

$$\mathrm{Ha} = aB\sqrt{\sigma_f/\mu} \tag{2}$$

$$N = \mathrm{Ha}^2/\mathrm{Re} \tag{3}$$

$$\mathrm{Re} = \rho v a/\mu. \tag{4}$$

When the Hartmann number and interaction parameter are sufficiently high, the majority of the flow is dominated by the balance between the pressure gradient and the electromagnetic force:

$$\nabla p = \boldsymbol{J}\times\boldsymbol{B}. \tag{5}$$

This is the primary force balance in the "core" region. The force balance equation must be supplemented by Ohm's law:

$$\boldsymbol{J} = \sigma_f(-\nabla\phi + \boldsymbol{v}\times\boldsymbol{B}) \tag{6}$$

the conservation equations:

$$\nabla\cdot\boldsymbol{v} = 0 \tag{7}$$

$$\nabla\cdot\boldsymbol{J} = 0 \tag{8}$$

and the electrical and fluid boundary conditions, in order to fully determine the velocity profiles in the core. In this analysis, the magnetic Reynolds number is assumed small, such that the magnetic field is exactly equal to the externally applied field. (If this were not true, an additional equation for $\boldsymbol{B}$ would be needed.)

Because of the unique properties of inviscid, inertialess MHD flow, the equations can be integrated along magnetic field lines to obtain expressions for the unknown current, velocity, and electric potential fields in terms of two-dimensional functions of integration which are constant along magnetic field lines. The functions of integration are determined through application of the boundary conditions at the surface of the pipe. In this way, the three-dimensional system of equations in eight unknowns, eqs. (5)–(8), can be transformed to a coupled set of (at most) four two-dimensional partial differential equations in four unknowns [1]. The primary difficulty in this approach results from the fact that the currents and velocities are specified in the natural coordinate system of the magnetic field, whereas the boundary equations (which determine the solution) depend on the geometry of the wall. This results in coordinate system transformations as an inherent part of the method.

The results of integration are as follows:

$$\boldsymbol{J}_\perp = \frac{\boldsymbol{B}}{B^2}\times\nabla p \tag{9}$$

$$J_\parallel = \int\left(\boldsymbol{B}\times\nabla\frac{1}{B^2}\right)\cdot\nabla p\ \mathrm{d}l + A_1 \tag{10}$$

$$\phi = -\int\int\left(\boldsymbol{B}\times\nabla\frac{1}{B^2}\right)\cdot\nabla p\ \mathrm{d}l\ \mathrm{d}l + A_1 l + A_2 \tag{11}$$

$$\boldsymbol{v}_\perp = -\frac{1}{\sigma_f B^2}\nabla p + \frac{\boldsymbol{B}}{B^2}\times\nabla\phi \tag{12}$$

$$v_\parallel = \int\left[\left(\boldsymbol{B}\times\nabla\frac{1}{B^2}\right)\cdot\nabla\phi + \frac{\nabla p}{\sigma_f}\cdot\nabla\frac{1}{B^2} + \frac{\nabla^2 p}{\sigma_f B^2}\right]\mathrm{d}l + A_3. \tag{13}$$

Equation (9) is obtained directly from a cross product of $\boldsymbol{B}$ with the pressure balance equation, eq. (5). Similarly, eqn. (12) is obtained directly from a cross product of $\boldsymbol{B}$ with Ohm's law. The parallel components of $\boldsymbol{J}$ and $\boldsymbol{v}$ are then found by integrating the conservation equations ((7) and (8)) along the magnetic field lines using the known perpendicular components. Finally, the potential is found by integrating the parallel current, using:

$$J_\parallel = -\frac{\partial\phi}{\partial l} \tag{14}$$

The variable l represents the distance along $\boldsymbol{B}$.

In order to express boundary conditions on the functions of integration, the functions of integration

(p, A_1, A_2, A_3) must be related to physical variables in the duct. For example, if the magnetic field lines define the x-direction, then (for the general, non-symmetric case) the four functions are replaced by $\phi_l(y, z)$, $\phi_r(y, z)$, $p(y, z)$, and $v_{x0}(y, z)$, where ϕ_l and ϕ_r refer to the potential evaluated at the left and right walls, p is the pressure (which does not vary along x), and v_{x0} is the x-component of velocity evaluated at $x = x_0$. These four functions are easily related to the original A_1, A_2, A_3, and p. For symmetric problems, only two functions are needed. These are chose to be $p(y, z)$ and $\phi(y, z)$, where ϕ can be evaluated at either wall or at some value of x.

The four boundary equations which determine the functions of integration are mass and current conservation expressed at the two walls which are intercepted by the field lines. For conducting ducts:

$$\boldsymbol{v} \cdot \hat{\boldsymbol{n}} = 0 \tag{15}$$

$$\Phi \nabla_w^2 \phi = \boldsymbol{J}_f \cdot \hat{\boldsymbol{n}}, \tag{16}$$

where $\Phi = \sigma_w t / \sigma_f a$ is the wall conductance ratio, J_f is the current density in the fluid, and the Laplacian, ∇_w^2, is performed in the wall only. Equation (16) follows from Ohm's law in the wall ($\boldsymbol{J}_w = -\sigma_w \nabla_w \phi$) and current conservation ($\nabla \cdot \boldsymbol{J}_w = 0$), where the right-hand side ($\boldsymbol{J}_f \cdot \hat{\boldsymbol{n}}$) is an effective source term coming from the fluid.

For insulating ducts, currents return through the Hartmann boundary layers, and current conservation is expressed as (see [1]):

$$\left(\frac{1}{\mathrm{Ha}} (\nabla \times \boldsymbol{v}) + \boldsymbol{J} \right) \cdot \hat{\boldsymbol{n}} = 0. \tag{17}$$

Boundary conditions are needed on the functions of integration at the edges of the computational grid. At the inlet and outlet, fully-developed conditions are applied: at the inlet $p = p_1$ and $\partial / \partial z = 0$, at the outlet $p = p_2$ and $\partial / \partial z = 0$.

The equations given above are very general. They apply to any duct shape with any conductivity and any magnetic field intensity and direction. The primary restriction is that each field line must pass through walls at no more than two points, and that the walls are smooth (the normal vector is continuous). If a field line passes through more that two points (such as at a wall parallel to the field) then additional information must be supplied to resolve the electric potential along the wall. This results in "side" layers. The second condition – discontinuous wall direction – results in internal shear layers. These special cases can be treated approximately; however, no further attempt is made to discuss them here.

3. Solution for a circular pipe with varying transverse and parallel magnetic field

The method described above has been used to solve for the pressures and velocity profiles in a circular pipe with a varying magnetic field having components in both the transverse and parallel directions with respect to the flow. Solutions were obtained using a finite difference approximation to the derivatives.

The geometry is shown in fig. 1. The magnetic field is given by:

$$\boldsymbol{B} = B_x(z)\,\hat{\boldsymbol{x}}. \tag{18}$$

The computational grid is in the natural coordinate system of the magnetic field. The pipe is placed at an angle, α, with respect to the magnetic field, resulting in both transverse and parallel components. The magnetic coordinate system is Cartesian (x, y, z) and the circular pipe wall is described by the angle θ and longitudinal distance λ.

When $\alpha = 0$, the field is entirely transverse. Extensive data have been taken at the ALEX facility for a conducting circular pipe in the entrance and exit region of a transverse magnetic field [5]. Comparisons have been made between the ALEX data and the direct integration method, and there is excellent agreement. To conserve space, only the axial pressure gradient and the transverse velocity profiles near the exit are presented here.

Figure 2 shows the normalized transverse magnetic field strength as a function of axial location, with $z = 0$

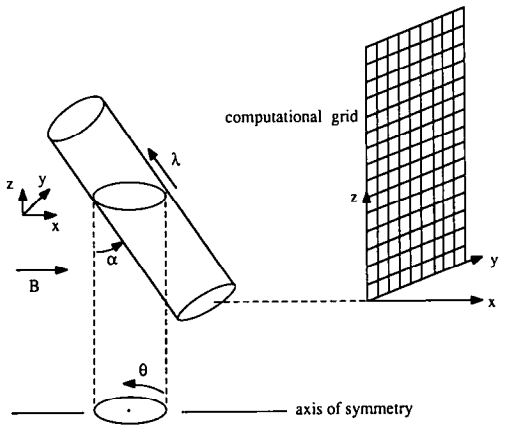

Fig. 1. Circular pipe geometry.

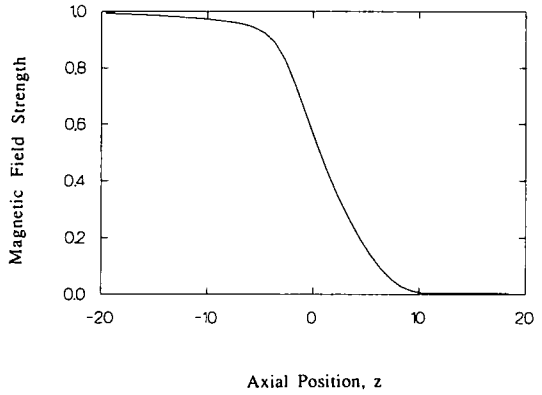

Fig. 2. Transverse magnetic field strength in ALEX.

located roughly at the point where the field drops to half of its maximum value. The wall conductance ratio is 0.026. In the experiment, Ha = 6400 and $N = 10{,}000$ (in the analysis, both are assumed infinite).

Figure 3 shows the experimental and calculated axial pressure gradient at $y = 0$ (the center for the pipe) and $y = 1$ (at the wall). The experimental pressure gradient is averaged over 6-inch intervals, which tends to smooth the non-uniformities. A noticeable "hump" exists just upstream of the exit at $y = 1$. This behavior is much more pronounced at $y = 0$, indicating the tendency for the flow to be retarded near the pipe center. The experimental data at $y = 0$ were obtained from a combination of the gradient at $y = 1$ and the transverse pressure difference between $y = 0$ and $y = 1$.

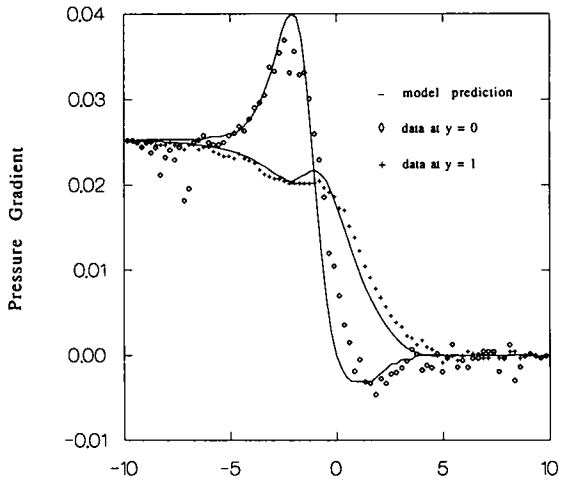

Fig. 3. Axial pressure gradient at $y = 0$ and $y = 1$: comparison with ALEX data.

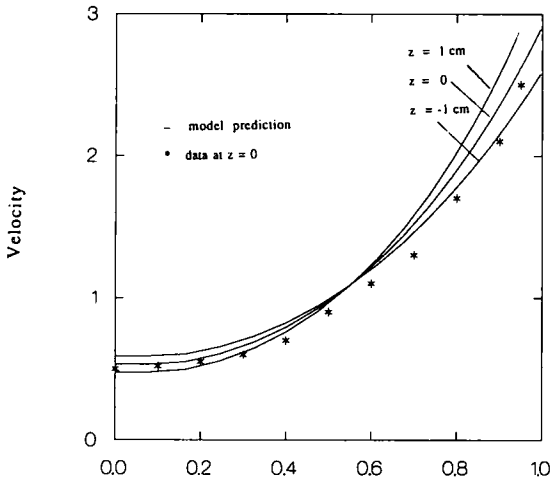

Fig. 4. Axial velocity near $z = 0$: comparison with ALEX data.

Figure 4 shows the longitudinal component of the velocity near the exit. The typical "M-shaped" profile is clearly seen. The calculated profile is shown shown 1 cm upstream and 1 cm downstream of the exit, indicating the rapid changes which occur there. All results are represented in dimensionless form, normalized by the

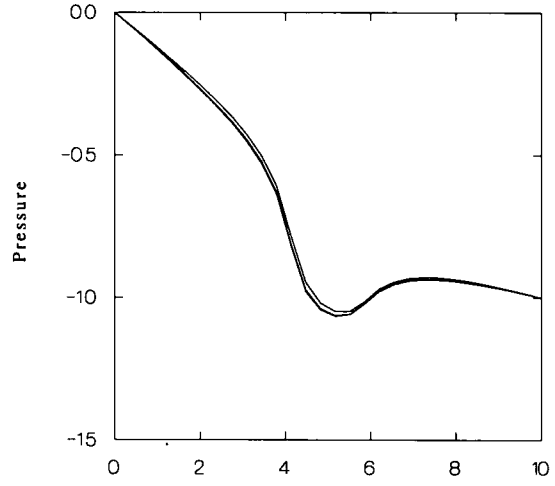

Fig. 5. Axial pressure profiles in the off-angle cylinder: $\alpha = 0$, 15, 30°.

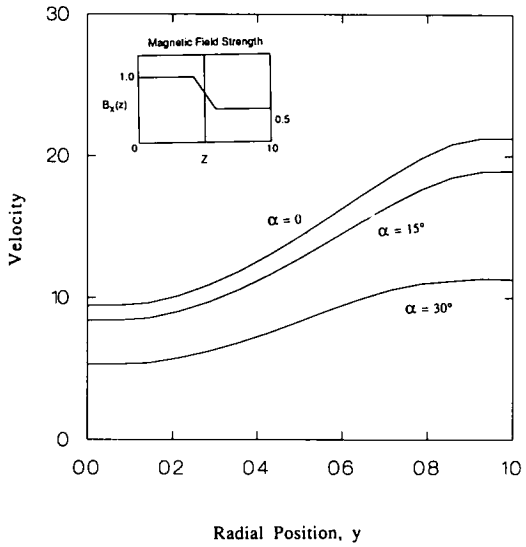

Fig. 6. Axial velocity profiles in the off-angle cylinder: $\alpha = 0$, 15, 30°.

maximum field strength, the pipe radius, the average velocity, and the conductivity of the fluid.

While experimental verification is not available, problems with $\alpha \neq 0$ have been examined. As an example, angles of 0, 15, and 30° were solved with a magnetic field strength changing from 1 to 0.5 over 1.5 pipe radii. Results are shown in figs. 5–7. Figure 5 shows that the axial pressure gradients are nearly identical of the three cases (given the same axial pressure difference applied across the pipes). However, as seen in figs. 6 and 7, the longitudinal and radial velocity profiles show significant differences. Higher angles result in lower bulk flow rates. Differences in the axial component of velocity are more pronounced than in the component normal to the wall.

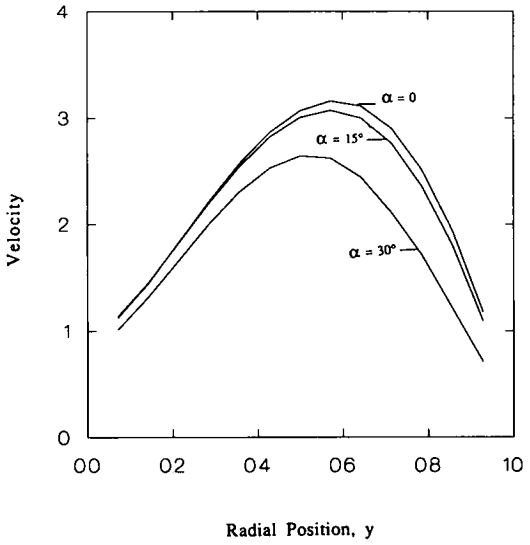

Fig. 7. Radial velocity profiles in the off-angle cylinder: $\alpha = 0$, 15, 30°.

4. Solution for a circular pipe with arbitrarily varying radius

Another problem solved using the direct integration method consists of a straight circular pipe with a smoothly varying radius located in a uniform transverse field. The geometry is shown in fig. 8. The radius is given by $R(z)$, where the z coordinate represents the axial distance along the pipe. In this case, symmetry leads to $A_1 = 0$ and $A_3 = 0$, and the unknowns are simply p and ϕ – the pressure and electric potential along the center plane of the pipe ($x = 0$).

The normal to the wall, used in eqs. (15) and (16), is determined from the slope of the pipe wall. The slope is given by $dR/dz = \gamma$, and the parameters β and δ, which are used in defining the normal, are given by:

$$\beta = \frac{1}{\sqrt{1 + 1/\gamma^2}} \tag{19}$$

$$\delta = \frac{1}{\sqrt{1 + \gamma^2}}. \tag{20}$$

(21)

Then the normal is expressed as:

$$\hat{n} = \hat{x}\delta \sin\theta - \hat{y}\delta \cos\theta + \hat{z}\beta. \tag{22}$$

Numerically, this system of equations is much easier to solve on a rectangular grid. In order to provide this, a

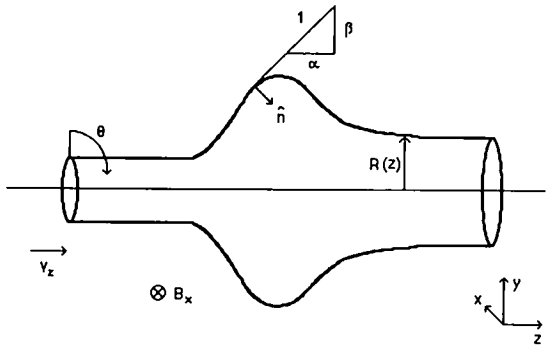

Fig. 8. Geometry for the variable-radius pipe.

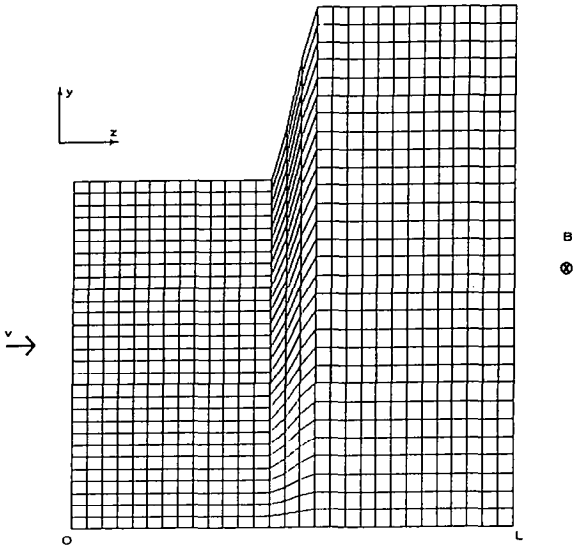

Fig. 9. Computational grid for the orifice expansion.

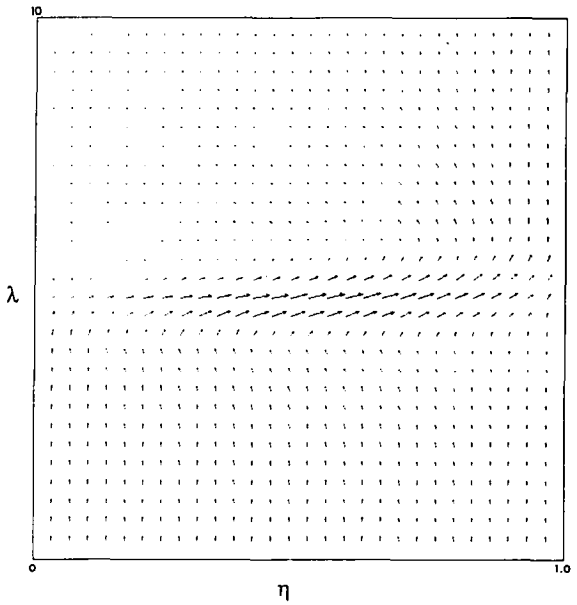

Fig. 11. Velocity vector field at $\chi = 0$ for the orifice expansion.

coordinate transformation was made to scale the radial coordinate such that it varies between 0 and 1. Rather than the $(y - z)$ plane, the $(\eta - \lambda)$ computational plane was used, where:

$$\eta = y/R(\lambda) \tag{23}$$

$$\lambda = z \tag{24}$$

$$\chi = x/R(\lambda). \tag{25}$$

The domain of the solution is now $\chi = 0$, $0 \leqslant \eta \leqslant 1$, and $0 \leqslant \lambda \leqslant L$.

A sample problem shown here is for a simple orifice expansion. The outlet radius is 1.5 times the inlet, with the expansion occurring over 1 pipe radius (see fig. 9). The wall conductance ratio is 0.005.

Figures 10 and 11 show the resulting pressure distribution and velocity vector field (at $x = 0$). The effect of the perturbation is restricted to within a few radii of the region in which the radius is changing.

The pressure varies linearly with λ throughout the bulk of the pipe. Near the perturbation, there is a deep well that is related to the vertical currents. The fluid is accelerated as it enters this region, and decelerated as it climbs up the back side. Near the pipe center, the velocity decreases nearly to zero. Theory predicts for a sufficiently low conductance ratio and rapid expansion that a recirculating eddy may form; however, this is not

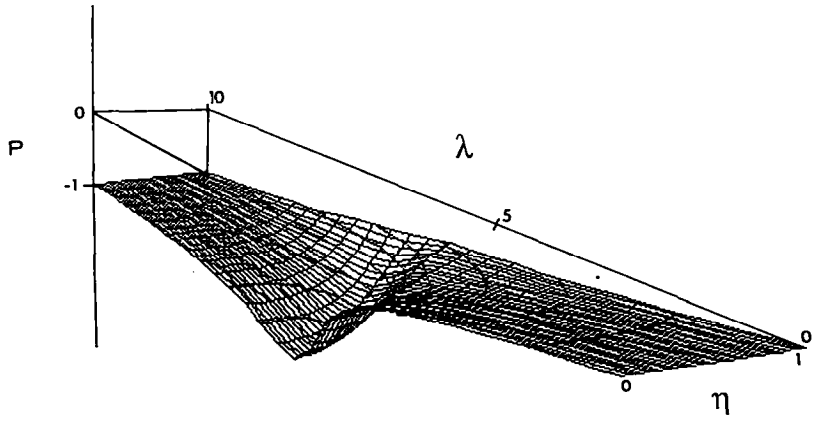

Fig. 10. Pressure profile for the orifice expansion.

observed in the present case. (Note: the scaling on the vector field plots tends to exaggerate the vertical component over the axial component. The aspect ratio of the pipe is 10 : 1.)

5. Concluding remarks

The core flow approximation greatly simplifies solution of the MHD equations. A general approach has been presented here which can, in principle, treat problems with great geometric complexity in both the magnetic field and the structure. Solutions have been obtained in circular conducting pipes with varying field strength, pipe radius, and angle between the field and the pipe axis. However, solutions for even more complex problems can and should be demonstrated before the full capabilities of the method can be assessed. Further work is also needed in order to fully understand the parameter ranges and geometries under which the core flow approximation is valid.

References

[1] A.G. Kulikovskii, Slow steady flows of a conducting fluid at large Hartmann numbers, Fluid Dynamics 3, 2 (1968) 3–10. (Izvestia Akademi Nauk SSSR, Mekhanika, Zhidkosti i Gaza).

[2] J.C.R. Hunt and J.A. Shercliff, Magnetohydrodynamics at high Hartmann number, Ann. Rev. Fluid Mech. 3 (1971) 37.

[3] J.C.R. Hunt and C.S.S. Ludford, Three-dimensional MHD duct flows with strong transverse magnetic fields. Part I: Obstacles in a constant area channel, J. Fluid Mech. 33 (1968) 693–714.

[4] J.S. Walker, Three-dimensional laminar MHD flows in rectangular ducts with thin conducting walls and strong transverse non-uniform magnetic fields, Liquid Metal Flows and Mangetohydrodynamics, (American Institute of Aeronautics and Astronautics, New York, 1983).

[5] B.F. Picologlou, C.B. Reed and P.V. Dauzvardis, Experimental and analytical investigations of magnetohydrodynamic flows near the entrance to a strong magnetic field, Fusion Technology, Vol. 10 (Nov. 1986).

[6] J.C.R. Hunt and R.J. Holroyd, Applications of laboratory and theoretical MHD duct flow studies in fusion reactor technology, Culham Laboratory, CLM-R169 (May 1977).

[7] J.S. Walker and G.S.S. Ludford, MHD flow in circular expansions with thin conducting walls, Int. J. Engng. Sci. 13 (1973) 261–269.